ISBN: 978-3-95450-231-8 ISSN: 2673-5490 doi: 10.18429/JACoW-IPAC2023-WEPL070

STATUS OF THE SOLEIL II ROBUSTNESS STUDIES

O. R. Blanco-Garcia*, A. Loulergue, L. S. Nadolski, R. Nagaoka, M.-A. Tordeux
Synchrotron SOLEIL, Saint-Aubin, France

Abstract

SOLEIL, the French third-generation synchrotron radiation facility, is in the TDR phase of its upgrade to a new fourth-generation synchrotron light source, called SOLEIL II. Its storage ring lattice design has evolved over the last year to better adjust its parameters taking into account the results of the mechanical integration, more realistic magnet design [1], and the geometrical constraints for the extraction of the photon beams. A new configuration of girders has been introduced, and the correction strategies have been refined. A new corrector budget and updated results with more statistics are presented in this paper.

INTRODUCTION

The SOLEIL II project aims to design and build a 2.75 GeV diffraction-limited synchrotron light source preserving the existing infrastructure, 29 beamlines (BLs) in the far-IR to hard X-rays, and the 500 mA uniform filling pattern. The lattice of the new storage ring presented in the Conceptual Design Report (CDR) [2, 3] is built over a non-standard combination of twelve 7BA cells and eight 4BA cells compliant with strong geometric constraints to produce a 84 pm rad natural emittance. The lattice can accommodate 20 straight sections (18 for insertion devices) where the betatron functions are minimized at their centers to be close to the matching values [2]. The injection uses a Multipole Injection Kicker (MIK) to inject the beam off-axis in the horizontal plane in a quasi-transparent way [4, 5], and a fall-back solution for early day beam commissioning using a 4-kicker injection bump option is also under consideration. During the Technical Design Report (TDR) phase two double-waist mini-beta sections were introduced with the addition of a quadrupole triplet at their centers and a magnetic chicane for one of them to host canted in-vacuum undulators leading to a new reference lattice [1, 6, 7]. The short straight sections have been extended in order to allow the use of the existing in-vacuum insertion devices (IVUs), the tunability of the lattice has been improved, first mechanical integration have been considered. Table 1 shows the main parameters without the harmonic cavity, and further details on the radio-frequency (RF) system can be found in [8, 9].

The robustness studies have been refined from the work done in the CDR phase [10]. The correction strategy for the TDR lattice is described in [11]. In this article, we show the corrector strengths and update the performance obtained from start-to-end simulations.

* oscar-roberto.blanco-garcia@synchrotron-soleil.fr

Table 1: Parameters of the Bare SOLEIL II TDR Lattice Without Harmonic Cavity

Parameter, **Units**	**Value**
Lattice	TDR V2366 SYM1
Energy, GeV	2.75
Circumference, m	353.970
Symmetry/Cell Number	1/20
H. Natural Emittance, pm rad	84
V. Emit. (30% H. Emit), pm rad	25
Tunes (H/V/L)	54.2/18.3/0.00214
Energy Spread, %	0.091
Bunch Length, ps	8.5
Harmonic Number	416
Main RF Frequency, MHz	352.327
Energy Loss per turn, keV	457
Main RF Voltage, MV	1.8
Natural Chromaticities H/V	-118.9/-55.0
Operation Chromaticities H/V	+1.6/+1.6
Momentum Compaction Factor	1.06×10^{-4}
Damping Time H/V/L, ms	7.9/14.1/12.2
Touschek Lifetime (500 mA), h	3.0

LATTICE CONFIGURATION

The lattice layout is shown in Fig. 1. It was modified to include a chicane in one of the two long straight sections. The girder number has been reduced from 214 to 86 (5 x 12 7BA, 3 x 8 4BA cells, 1 x 2 triplets) which improves the magnet positioning correlation and should be beneficial in reducing the lattice perturbation. The magnet and girder roll angles have been updated from the previous definition [11] to 100 (2σ-cut) and 60 (1σ-cut) µrad RMS for magnets and girders, respectively. The lattice contains 180 Beam Position Monitors (BPM) distributed along the machine with one BPM per unit cell, two BPMs on each side of a straight section, and two BPMs per triplet in two of the twenty straight sections.

To correct the closed orbit with this BPM configuration, 180 dipolar correctors dedicated to the slow orbit correction are included: one horizontal and one vertical corrector per unit cell and two correctors on each side of every straight section in locations with large optics β functions, plus two per triplet in locations given by the sextupoles. Optics correction is performed using 196 standalone quadrupole correctors and 216 quadrupolar coils in octupoles for a total of 412 correctors. A subset of 136 octupoles will have a skew quadrupole coil for coupling correction (see Table 2).

ISBN: 978-3-95450-231-8 ISSN: 2673-5490 doi: 10.18429/JACoW-IPAC2023-WEPL070

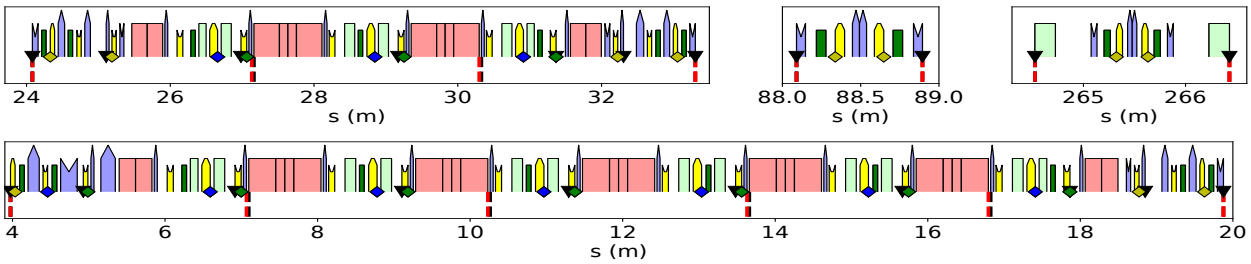

Figure 1: Layout of the SOLEIL II TDR lattice with (top-left) 4BA, (bottom) 7BA arc cells, (top center) mini-beta section without chicane, and (top right) with chicane. Permanent dipoles and reverse bends are shown in light-red and in light green, respectively. Sextupoles are in yellow, where 180 of which have a dipolar corrector and are marked with a colored diamond at their feet (blue for horizontal, green for vertical, and yellow for correctors in both planes). Quadrupoles are shown in light blue and octupoles in dark green; all 216 octupoles and 196 electromagnetic quadrupoles (412 in total), each one aside of a sextupole, are used for linear optics corrections, while a subset of 180 near a dipolar corrector is used for BBA. The BPMs are shown as black triangles. Girder extremities are shown as black (start) and red (end) marks.

Table 2: Girders, BPMs, and Corrector Summary

Number	Symbol	Element
86	—	Girder
180	BPM	Beam Position Monitor
180/180	θ_x/θ_y	Hor/Ver dipolar corrector
412/136	Q_n/Q_t	Normal/Skew quadrupole corr.

CORRECTION STRATEGY UPDATE

The initial lattice was modified to include girders, BPMs, correctors, and their errors using the Simulated Commissioning (SC) toolbox [12, 13]. The beam dynamics is simulated with AT [14, 15], optics corrections use Linear Optics from Closed Orbits (LOCO) [16]. Parallel computation resources are set up using the job scheduler SLURM [17] and Matlab [18]. Jupyter [19], Pandas [20], Seaborn [21], Matlab and, pyAT [22] are used for data analysis.

Statistical results have been refined from typical commissioning from 30 to 100 rings which also increases the confidence in the machine parameter recovery. The physical aperture has also been modeled to account for IVU apertures. Dynamic Aperture (DA) and Momentum Aperture (MA) calculations have been refined to include the 6D closed orbit. BPM errors are fully included in the start-to-end of commissioning simulations.

Corrections have also evolved: the Beam Based Alignment (BBA) procedure is performed using a combination of standalone quadrupole correctors and quadrupolar coils of octupole magnets; BBA is done on a different set of magnets in each plane, here called *hybrid BBA*; the LOCO procedure uses the dedicated quadrupoles and quadrupolar coils on octupoles; decapolar error components in sextupoles with dipolar coils have been included in the beam dynamics simulations. Sextupoles were kept on from the first day of commissioning, with the possibility to turn them off to gain DA for a static energy error from injection below 0.1%.

Each ring in the simulation will follow a step-by-step based procedure in order to restore the beam parameters: A) *On-axis* injection and trajectory correction up to first-turn correction, second-turn correction, and convergence, B) Tuning of the main RF system to store the beam which gives the first closed orbit (CO), C) closed orbit BBA and orbit correction, D) LOCO. If necessary, E) Iterations of BBA, LOCO, and orbit correction to improve the DA, thus, increasing the injection efficiency f) Final performance evaluation.

On the other hand, many simplifications still prevail: dipolar correctors are foreseen to be constructed as extra coils in 180 sextupole magnets, however, they are simulated as perfectly aligned and calibrated additional elements next to sextupole magnets; the LOCO procedure does not fit the BPM roll errors; the effect of longitudinal errors and insertion devices has been estimated independently in a case-by-case manner but not integrated to the start-to-end simulation; static multipolar components on the magnets have also been included in particular cases but not for these results; local bumps inside the arcs might be required but not studied; simulations still skip the iterations mentioned in E); at last, the simulation model contains only the main RF cavity and does not include any bunch lengthening effect from the resistive wall or the harmonic cavity.

Corrector Budget

The 100 simulated machines pass through all simulation stages from one-turn correction to beam capture, and BBA for final orbit correction.

The dipolar corrector strength budget for orbit correction is shown in Table 3. It is necessary to provide additional corrector strength for steering the source points of the BLs (where a 100 µm bump in a straight section would require up to 420 µrad), for beam-based measurement, slow drift, ID feedforward, permanent magnet errors, slow drifts with temperature or long term slab settlement. All of this points to the need to increase the dipolar correctors, in particular in the straight sections.

The table 3 also shows the normal and skew correctors budget required by LOCO to correct the optics for 99 machines. Quadrupolar correctors will also be used to com-

ISBN: 978-3-95450-231-8 ISSN: 2673-5490 doi: 10.18429/JACoW-IPAC2023-WEPL070

pensate for the perturbation induced by the insertion which has been estimated through particular cases to require an additional 0.15 to 0.6 T depending on the studied insertion configuration.

Table 3: Peak Strength of the Dipolar and Quadrupolar Correctors for Orbit and Optics Correction

Peak Strength	Max Design	Percentile 100	95	90	68	50
$\|\theta_x\|$ (µrad)	450-700	486	401	385	333	303
$\|\theta_y\|$ (µrad)	450-700	301	278	267	237	223
$\|Q_n\|$ (mT)	600	581	467	431	363	335
$\|Q_t\|$ (mT)	600	224	186	173	157	147

Table 4 shows the optical function beats obtained after the application of the correctors to the simulated rings. Peak values are particularly large, and would require further study to consider methods to reduce them.

Table 4: Optics Beat in Peak and RMS Values

Value	Units	Percentile 100	95	90	68	50
peak		**100**	**95**	**90**	**68**	**50**
$\|\Delta\beta_x/\beta_x\|$	(%)	7.89	5.59	5.36	4.74	4.38
$\|\Delta\beta_y/\beta_y\|$	(%)	7.59	5.21	4.81	3.94	3.56
$\|\Delta\eta_x\|$	(mm)	2.28	1.19	1.14	0.97	0.87
$\|\Delta\eta_y\|$	(mm)	0.87	0.79	0.75	0.63	0.58
rms		**100**	**95**	**90**	**68**	**50**
$\|\Delta\beta_x/\beta_x\|$	(%)	1.13	0.90	0.85	0.75	0.70
$\|\Delta\beta_y/\beta_y\|$	(%)	1.16	0.89	0.81	0.68	0.63
$\|\Delta\eta_x\|$	(mm)	0.37	0.22	0.20	0.17	0.15
$\|\Delta\eta_y\|$	(mm)	0.13	0.11	0.11	0.10	0.10

Amplification Factors and Hybrid BBA

Because of the reduced number of BPMs with respect to the number of magnets in the lattice, and given the very large strength of the quadrupoles and sextupoles, even a small residual closed orbit of tens of micrometers would still produce a large perturbation which creates both the large peak optics-beat and the high corrector strengths. This is more easily understood through the amplification factors [23] shown in Fig. 2. The BBA is able to mitigate some, but not all, of the amplification factors along the arcs. In the unit cell the largest component occurs at different magnets per plane, which leads to performing the so-called *hybrid* BBA.

CORRECTION PERFORMANCE

Figure 3 shows the restoration of the DA, and Table 5 the Touschek lifetime of the rings. The machines achieve more than -4 mm of horizontal DA, which increases the likelihood of off-axis injection efficiency wrt previous results. The recovered momentum aperture is able to restore the Touschek lifetime up to 2.0 h for the median of the machines.

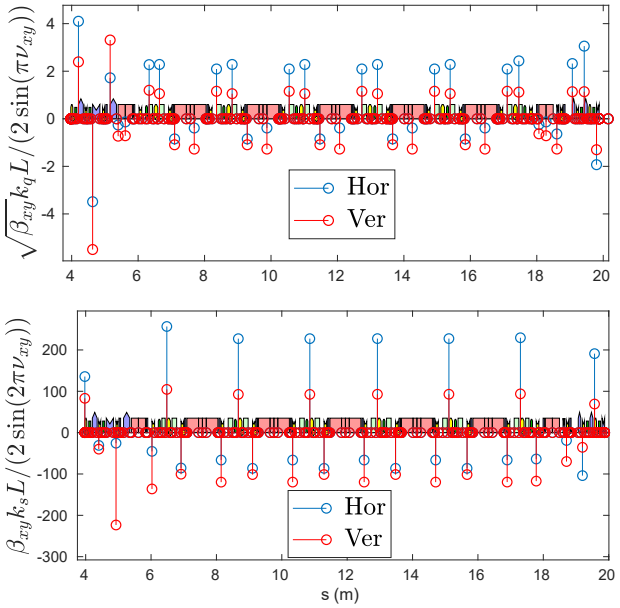

Figure 2: Example of a 7BA (top) quadrupolar and (bottom) sextupolar amplification factors.

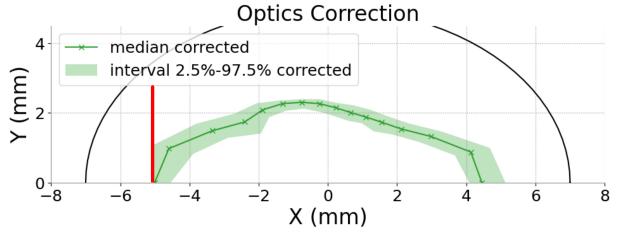

Figure 3: Dynamic aperture at the injection point of the lattice. Physical aperture in black, and thin septum in red.

Table 5: Touschek Lifetime Without Harmonic Cavity for the Design Lattice and 99 Corrected Surviving Machines

Design	Unit	Percentile 100	90	68	50	32	10
3.0	(h)	2.6	2.3	2.2	2.0	1.9	1.8

CONCLUSION

The SOLEIL II project has updated its lattice design over the last year. The robustness studies have evolved to include more detailed simulations of the commissioning steps and higher statistics. A mean Touschek lifetime of 2±0.2 h is recovered without harmonic cavity. The dynamic aperture is recovered and allows to study off-axis injection. Corrector budget values for orbit and optics correction are reported. The SOLEIL II alignment strategy will be reviewed to reduce the impact of the strong sextupoles and permanent quadrupoles on the corrector budget. In addition, the corrector strengths will be increased to save marge to meet the needs of multiple use cases. The commissioning simulations will continue to adapt to the study of longitudinal errors, off-axis injection, insertion devices, and others mentioned.

ISBN: 978-3-95450-231-8 ISSN: 2673-5490 doi: 10.18429/JACoW-IPAC2023-WEPL070

REFERENCES

[1] C. Kitegi *et al.*, "Magnet design status of SOLEIL II", presented at the IPAC'23, Venice, Italy, May 2023, paper WEPM048, this conference.

[2] Synchrotron SOLEIL, "Conceptual Design Report (CDR) SOLEIL Synchrotron Upgrade", L'Orme des Merisiers, Saint-Aubin, France. https://www.synchrotron-soleil.fr/fr/file/13803/download?token=OUzsp46P

[3] A. Nadji and L. S. Nadolski, "Upgrade Project of the SOLEIL Accelerator Complex", Synchrotron Radiation News, 36:1, 10-15, doi:10.1080/08940886.2023.2186661

[4] R. Ollier *et al.*, "Performance Report of the SOLEIL Multipole Injection Kicker", in *Proc. IPAC'22*, Bangkok, Thailand, Jun. 2022, pp. 2675–2678. doi:10.18429/JACoW-IPAC2022-THPOPT039

[5] R. Ollier, *et al*, "Toward transparent injection with a multipole injection kicker in a storage ring", *Phys. Rev. Accel. Beams*, vol. 26, p. 020101, Feb. 2023. doi:10.1103/PhysRevAccelBeams.26.020101

[6] A. Loulergue *et al.*, "TDR Baseline Lattice for the Upgrade of SOLEIL", in *Proc. IPAC'22*, Bangkok, Thailand, Jun. 2022, pp. 1393–1396. doi:10.18429/JACoW-IPAC2022-TUPOMS004

[7] A. Loulergue *et al.*, "TDR Baseline Lattice for SOLEIL II Upgrade Project", presented at the IPAC'23, Venice, Italy, May 2023, paper MOPM031, this conference.

[8] A. Gamelin, W. Foosang, P. Marchand, R. Nagaoka, and N. Yamamoto, "Beam Dynamics with a Superconducting Harmonic Cavity for the SOLEIL Upgrade", in *Proc. IPAC'22*, Bangkok, Thailand, Jun. 2022, pp. 2229–2232. doi:10.18429/JACoW-IPAC2022-WEPOMS003

[9] N. Yamamoto, A. Gamelin, P. Marchand, R. Nagaoka, and S. Sakanaka, "Stability Survey of a Double RF System with RF Feedback Loops for Bunch Lengthening in a Low-emittance Synchrotron Ring", presented at the IPAC'23, Venice, Italy, May 2023, paper WEPL161, this conference.

[10] D. Amorim, A. Loulergue, L. S. Nadolski, and R. Nagaoka, "Robustness Studies and First Commissioning Simulations for the SOLEIL Upgrade Lattice", in *Proc. IPAC'21*, Campinas, Brazil, May 2021, pp. 171–174. doi:10.18429/JACoW-IPAC2021-MOPAB038

[11] O. R. Blanco-García, D. Amorim, M. A. Deniaud, A. Loulergue, L. S. Nadolski, and R. Nagaoka, "Status of the Soleil Upgrade Lattice Robustness Studies", in *Proc. IPAC'22*, Bangkok, Thailand, Jun. 2022, pp. 433–436. doi:10.18429/JACoW-IPAC2022-MOPOTK004

[12] T. Hellert et al., "Toolkit for simulated commissioning of storage-ring light sources and application to the advanced light source upgrade accumulator", *Phys. Rev. Accel. Beams*, vol. 22, p. 100702, 2019. doi:10.1103/PhysRevAccelBeams.22.100702

[13] Toolkit for Simulated Commissioning (SC), https://sc.lbl.gov/.

[14] G. J. Portmann, W. J. Corbett, and A. Terebilo, "An Accelerator Control Middle Layer Using Matlab", in *Proc. PAC'05*, Knoxville, TN, USA, May 2005, paper FPAT077, pp. 4009–4011.

[15] AT: Accelerator Toolbox is collection of tools to model storage rings and beam transport lines in MatLab, http://atcollab.sourceforge.net/index.html

[16] J. Safranek, G. Portmann, A. Terebilo. "MATLAB-base LOCO", in *Proc. of EPAC 2002*, Paris, France, pp. 1184–1186.

[17] SLURM: an open source, fault-tolerant, and highly scalable cluster management and job scheduling system for large and small Linux clusters, https://slurm.schedmd.com/.

[18] MatLab, https://mathworks.com/.

[19] Jupyter: Free software, open standards, and web services for interactive computing across all programming languages, https://jupyter.org/.

[20] Pandas: A fast, powerful, flexible and easy to use open source data analysis and manipulation tool, built on top of the Python programming language, https://pandas.pydata.org/.

[21] Seaborn: Statistical data visualization, https://seaborn.pydata.org/.

[22] Python Accelerator Toolbox: is a code used for simulating particle accelerators, used particularly for synchrotron light sources, https://pypi.org/project/accelerator-toolbox

[23] A. W. Chao, K. H. Mess, M. Tigner, and F. Zimmermann, *Handbook of accelerator physics and engineering*, Second Edition, World Scientific, 2013. doi:10.1142/8543